

The Effectiveness of LDPC Decoding Algorithms in 5G Channel Modelling of MIMO-OFDM System under the Influence of Spatial Correlation

Nguyen Thu Nga

Hanoi University of Science and Technology, Hanoi, Vietnam

**Email: nga.nguyenthul@hust.edu.vn*

Abstract

This paper investigates the spatial cross-correlation properties of 5G channel modeling in non-line of sight (NLOS) of Urban Micro Cell (UMi), Rural Macro Cell (RMa) and Indoor Cell (InH) at 6 GHz frequency band as Third Generation Partnership Project (3GPP) specification. In our spatial correlation Multiple-input multiple-output (MIMO) channel, when increasing the distances of BS antenna elements, the correlation characteristics of the channel dramatically vary, which leads to altering the observed system behavior. By analyzing the 5G LDPC code and using different decoding algorithms and code rates, we evaluate the system's performance by Bit Error Rate (BER) in a wideband correlated Multiple-input multiple-output Orthogonal Frequency Division Multiplexing (MIMO-OFDM) system. In our spatial correlation, the more rising of the distances of antenna elements on the BS side, the better the effectiveness of the LDPC decoding algorithms achieved. Of the Belief Propagation based (BP-based) Algorithm, Offset Minimum-Sum (OMS) Algorithm and Linear Approximation Minimum-Sum (LAMS) Algorithm, we propose to use the LAMS decoding algorithm with a high code rate of 5/6 in our spatial correlated wideband channel because of lower complexity and more efficiency in term of the system's performance.

Keywords: MIMO-OFDM, 5G channel modeling, spatial cross-correlation, LDPC, LDPC decoding algorithm.

1. Introduction

The channel modelling simulators for each generation of mobile networks define the environment for the transmission of the wireless signal. The correlation properties of the channel modelling have been studied in [1] by 4G Long Term Evolution Advanced (LTE-A) standard in two kinds of channel modelling simulators: the geometry-based stochastic model (GBSM) and the parametric stochastic model (PSM). The 3GPP and ETSI have launched Standardization of Channel Modelling for 5G systems [2] in many propagation environments at frequency ranging from 0.5 GHz to 100 GHz. The new channel modelling simulators for 5G systems, such as massive MIMO, vehicle-to-vehicle, high-speed train and millimeter-wave (mm-Wave) have been introduced in [3] in different terms of either irregular-shaped GBSM or regular-shaped GBSM, as well as non-geometrical stochastic model (NGSM) or ray tracing (RT)/ ray launching (RL) methods.

The 3D MIMO channel space-time correlation functions for a fixed-to-mobile MIMO system in mm-Wave in Rayleigh and Rician narrow band channels have been presented in [4]. The 3-D statistical channel model [5] is simulated at a 28 GHz local area for narrow band MIMO system by studying the exponential spatial auto correlation of multipath component amplitudes. New spatial correlation expressions for rectangular arrays of cross-polarized

antennas [6] with 3D and 2D channel models have been analyzed by the accuracy of decomposing 3D channel capacity. The simulation is conducted in narrow band Rayleigh channel.

For frequencies from 6 GHz to 100 GHz, authors [7, 8] describe an initial 3D channel model in typical UMi, urban macro-cells (UMa), indoor offices and shopping malls, derived from extensive measurements across a multitude of bands. These researches show frequency dependence of the path loss as well as increased occurrence of blockage by the delay spread, the angular spread and the multi-path richness. The large-scale propagation path loss model is used over the entire microwave and mm-Wave frequency from 2 to 73 GHz with wave distances from 4 to 1238 m.

LDPC code is one kind of channel coding because of its capacity-approaching performance and low-complexity parallel decoding suitable for hardware implementation. The new radio of 3GPP defines the types of LDPC for 5G in [9]. The LDPC code [10] is studied in additive white Gaussian noise (AWGN) channel for 5G while many LDPC decoding algorithms [11] were deployed in machine learning. From the traditional Belief Propagation (BP) decoding, authors in [12] proposed the BP-based algorithm decoding in AWGN channel in term of utilizing normalization to improve the accuracy of the soft values.

LDPC code for MIMO-OFDM system [13, 14] has been studied with different decoding techniques to investigate the performance of the system without the channel modelling simulator. The MIMO-OFDM system is simulated under the WLAN standard or the white Gauss noise channel model in narrow band. That is, the MIMO-OFDM system's performance is not considered in both terms of the wideband frequency selective channel and spatial correlation channel of the 5G channel simulator. The system performance of MIMO-OFDM system in the case of using LDPC decoding algorithm, hence, is not investigated in the channel modelling simulator as the 5G channel of 3GPP.

Therefore, our work presents a studying of LDPC decode algorithm in the spatial cross-correlation of 5G channel modelling simulators in wideband 2×2 MIMO-OFDM system. The environments are NLOS UMi, NLOS RMa and NLOS InH cells at a frequency wideband of 6 GHz. The distances of antenna elements in the base station (BS) and mobile station (MS) sides are derived from the correlation results. We simulated the different LDPC decode algorithms with code rates in order to estimate the effectiveness of channel decoding in correlated MIMO-OFDM system. Our paper is presented in the structure as followings: the properties of spatial correlation of 5G channel modelling in NLOS case are computed in part 2. Next the algorithms of the LDPC decode are in part 3. Part 4 is the simulation results in the 2×2 MIMO-OFDM system and finally, the conclusions are given in part 5.

2. The Cross Spatial Correlation Function of the 5G Channel Model in Case of NLOS Scenario

This Cartesian coordinate system [2] with the spherical angles is represented by the zenith angle θ and the azimuth angle ϕ in Fig. 1. Authors translate between the Global Coordinate System (GCS) where the multiple BSs and MSs are used and Local Coordinate System (LCS) where an array antenna is used given by the bearing, the down-tilt and the slant angle.

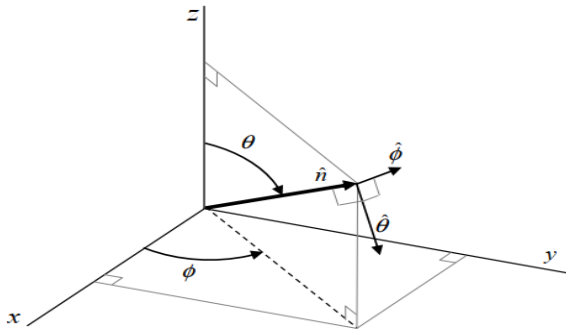


Fig. 1. The Cartesian coordinate system [2]

Our paper simulated the scenarios [2] of 5G channel modeling in NLOS case listed as follows:

- 1) UMi scenario in street canyon, open area at the width of 50 to 100 meters.
- 2) RMa scenario in the larger and continuous coverage rural with supporting high-speed vehicles and noise - limited.
- 3) Indoor scenario in the office environments and shopping malls.

The 3GPP defined that the impulse response function of wideband 5G channel modeling depends on the antenna element on both sides, the sub-paths are described [2] as:

$$h_{u,s}^{NLOS}(\tau, t) = \sum_{n=1}^2 \sum_{i=1}^3 \sum_{m \in R_i} h_{u,s,n,m}^{NLOS}(t) \delta(\tau - \tau_{n,i}) + \sum_{n=3}^N h_{u,s,n}^{NLOS}(t) \delta(\tau - \tau_n) \quad (1)$$

where n and m denote a cluster and a ray within each cluster, respectively; the mobile velocity vector v with travel azimuth angle ϕ_v , elevation angle θ_v , the τ is defined as the delay of each path to the receiver.

The $h_{u,s,n,m}^{NLOS}(t)$ [2] in (2) is the impulse response function (IRF) of two clusters that have the highest power ($n = 1, 2$), the paths are divided into three sub-clusters ($i = 1, \dots, 3$), each sub-cluster has each delay as can be seen in Table 1. The $h_{u,s,n}^{NLOS}(t)$ [2] in (3) is the IRF of MIMO channel with $n = 3, 4 \dots N$.

Whereas the $F_{rx,u}$; $F_{tx,s}$ are the radiation field of the receive and transmit antenna element, respectively; $\hat{r}_{rx,n,m}^T$ and $\hat{r}_{tx,n,m}^T$ are the spherical unit vector of AoA and AoD, respectively; n and m denote a cluster and a ray within each cluster, respectively; $\bar{d}_{rx,u}$, $\bar{d}_{tx,s}$ are the located vectors of antenna element u, s ; $\kappa_{n,m}$ is the cross polarisation power ratio in linear scale; λ_0 is the wavelength of the carrier frequency, the mobile velocity vector v with travel azimuth angle ϕ_v , elevation angle θ_v ; the $\Phi_{n,m}$ is the initial phases for each ray m of each cluster n in different polarization combinations of θ, ϕ angles.

Table 1. The sub-cluster information [2]

Sub-cluster i	Mapping to Rays R_i	Power $ R_i/M $
$i = 1$	$R_1 = 1 - 8; 19; 20$	10/20
$i = 2$	$R_2 = 9 - 12; 17; 28$	6/20
$i = 3$	$R_3 = 13 - 16$	4/20

$$h_{u,s,n,m}^{NLOS}(t) = \sqrt{\frac{P_n}{M}} \begin{bmatrix} F_{rx,u,\theta}(\theta_{n,m,ZOA}, \phi_{n,m,AOA}) \\ F_{rx,u,\phi}(\theta_{n,m,ZOA}, \phi_{n,m,AOA}) \end{bmatrix}^T \begin{bmatrix} e^{j\Phi_{n,m}^{\theta\theta}} & \sqrt{\kappa_{n,m}^{-1}} e^{j\Phi_{n,m}^{\theta\phi}} \\ \sqrt{\kappa_{n,m}^{-1}} e^{j\Phi_{n,m}^{\phi\theta}} & e^{j\Phi_{n,m}^{\phi\phi}} \end{bmatrix} \times \begin{bmatrix} F_{tx,s,\theta}(\theta_{n,m,ZOD}, \phi_{n,m,AOD}) \\ F_{tx,s,\phi}(\theta_{n,m,ZOD}, \phi_{n,m,AOD}) \end{bmatrix} \times \exp\left(\frac{j2\pi(\hat{r}_{rx,n,m}^T \times \bar{d}_{rx,u})}{\lambda_0}\right) \times \exp\left(\frac{j2\pi(\hat{r}_{tx,n,m}^T \times \bar{d}_{tx,s})}{\lambda_0}\right) \times \exp\left(\frac{j2\pi(\hat{r}_{rx,n,m}^T \times \bar{v})}{\lambda_0} t\right) \quad (2)$$

$$h_{u,s,n}^{NLOS}(t) = \sqrt{\frac{P_n}{M}} \times \sum_{m=1}^M \begin{bmatrix} F_{rx,u,\theta}(\theta_{n,m,ZOA}, \phi_{n,m,AOA}) \\ F_{rx,u,\phi}(\theta_{n,m,ZOA}, \phi_{n,m,AOA}) \end{bmatrix}^T \begin{bmatrix} e^{j\Phi_{n,m}^{\theta\theta}} & \sqrt{\kappa_{n,m}^{-1}} e^{j\Phi_{n,m}^{\theta\phi}} \\ \sqrt{\kappa_{n,m}^{-1}} e^{j\Phi_{n,m}^{\phi\theta}} & e^{j\Phi_{n,m}^{\phi\phi}} \end{bmatrix} \times \begin{bmatrix} F_{tx,s,\theta}(\theta_{n,m,ZOD}, \phi_{n,m,AOD}) \\ F_{tx,s,\phi}(\theta_{n,m,ZOD}, \phi_{n,m,AOD}) \end{bmatrix} \times \exp\left(\frac{j2\pi(\hat{r}_{rx,n,m}^T \times \bar{d}_{rx,u})}{\lambda_0}\right) \times \exp\left(\frac{j2\pi(\hat{r}_{tx,n,m}^T \times \bar{d}_{tx,s})}{\lambda_0}\right) \times \exp\left(\frac{j2\pi(\hat{r}_{rx,n,m}^T \times \bar{v})}{\lambda_0} t\right) \quad (3)$$

The transfer function $H(\cdot)$ in frequency domain is the Fourier transform of $h(\cdot)$ the channel impulse response and is calculated with τ_n - the delay of the n cluster:

$$H_{u,s}(f, t) = \sum_{n=1}^N h_{u,s}(\tau, t) \times e^{-j2\pi\tau_n f} \quad (4)$$

The spatial-temporal correlation function of 2×2 MIMO system is calculated by the time average operator as follows with λ_0 - the wavelength of the carrier frequency and $\Delta\bar{d}_{rx,u}, \Delta\bar{d}_{tx,s}$ or the $\Delta d_u, \Delta d_s$ are the distances of antenna elements u, s in the MS and BS side:

$$\begin{aligned} \rho(\Delta d_u, \Delta d_s, \Delta t) &= \rho(\Delta\bar{d}_{rx,u}, \Delta\bar{d}_{tx,s}, \Delta t) \\ &= \langle H_{u_1, s_1}(f, t) \times H_{u_2, s_2}^*(f, t + \Delta t) \rangle \\ &= \sum_{n=1}^N \sqrt{\frac{P_n}{M}} \sum_{m=1}^M \left(\begin{aligned} & \times \frac{j2\pi(\hat{r}_{rx,n,m}^T \times \Delta\bar{d}_{rx,u})}{\lambda_0} \\ & \times \frac{j2\pi(\hat{r}_{tx,n,m}^T \times \Delta\bar{d}_{tx,s})}{\lambda_0} \\ & \times \frac{j2\pi(\hat{r}_{tx,n,m}^T \times \bar{v})}{\lambda_0} \Delta t \end{aligned} \right) \quad (5) \end{aligned}$$

Set $\Delta t = 0$, the cross spatial correlation function depended on the distances of antenna elements in both sides of the 2×2 MIMO channel is presented as:

$$\begin{aligned} \rho(\Delta d_u, \Delta d_s) &= \rho(\Delta\bar{d}_{rx,u}, \Delta\bar{d}_{tx,s}) \\ &= \sum_{n=1}^N \sqrt{\frac{P_n}{M}} \sum_{m=1}^M \left(\begin{aligned} & \times \frac{j2\pi(\hat{r}_{rx,n,m}^T \times \Delta\bar{d}_{rx,u})}{\lambda_0} \\ & \times \frac{j2\pi(\hat{r}_{tx,n,m}^T \times \Delta\bar{d}_{tx,s})}{\lambda_0} \end{aligned} \right) \quad (6) \end{aligned}$$

For three UMi, RMa, InH environments NLOS case, Fig. 2 is the spatial correlation graph in the transmitter BS side when setting $\Delta d_u = 0\lambda$. In the case of $\Delta d_u = 0.5\lambda$, the correlation shapes are similar in three scenarios with the high amplitude and the minimum correlation values are around 0.45λ . In the case of $\Delta d_u = 10\lambda$, there were similar shapes, amplitudes and the minimum correlation values are around 0.3λ to 0.5λ . From that, in increasing the antenna elements of MS side, the minimum correlation values do not differ much from each other. The minimum correlation values (MCV) of three scenarios are similar to each other at the point of no correlation between antenna elements. We have the obtained MCVs from the results which have been given in Table 2.

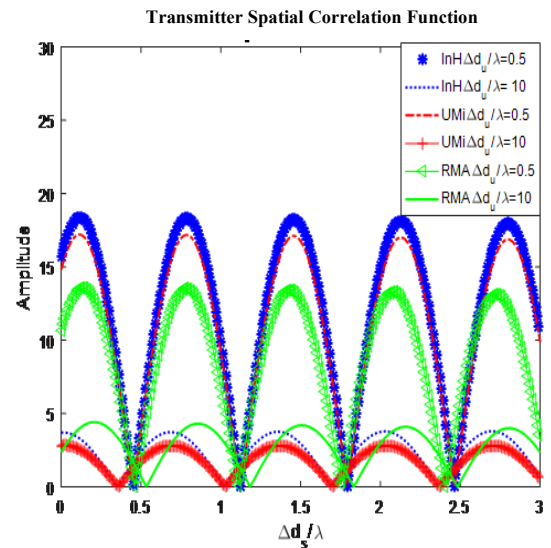


Fig. 2. The spatial correlation properties in BS side

Table 2. The min correlation value (MCV) in BS side

Envi	Δd_u	UMi ($\Delta d_s/\lambda$)	RMa ($\Delta d_s/\lambda$)	InH ($\Delta d_s/\lambda$)
MCV	0.5λ	0.4505	0.4605	0.4505
	10λ	0.36	0.531	0.3504

Table 3. The min correlation value in MS side

Envi	Δd_s	Umi ($\Delta d_u/\lambda$)	RMa ($\Delta d_u/\lambda$)	InH ($\Delta d_u/\lambda$)
MCV	10λ	0.3604	0.6607	0.3505
	16λ	0.4505	0.7808	0.4605

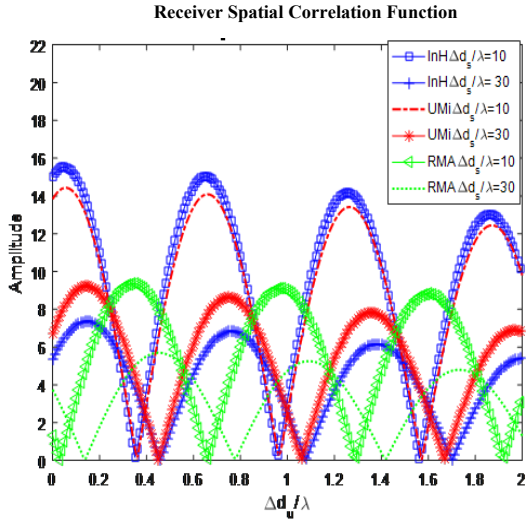


Fig. 3. The spatial correlation properties in MS side

Fig. 3 is the graph of spatial correlation in the receiver MS side when setting $\Delta d_s = 0\lambda$. In the three propagation environments, when Δd_s is changed from 10λ to 16λ , there were similar correlation shapes with MCVs in the range of 0.35λ to 0.66λ . MCVs of RMA environment are more variable than others, from 0.48λ to 0.66λ while in UMi and InH scenarios the MCVs are nearly the same values as each other. The MCVs of changing the $\Delta d_u/\lambda$ are described as in Table 3.

In spite of close shapes, the MS antenna element's distances are increased 20 times, the MCVs are nearly close to each other as in Fig. 2. However, in Fig. 3, if the BS antenna element's distances rise 1.5 times more than each other, there were much more alterations in terms of correlation coefficients. Therefore, from mentioned analysis, the more varying the space of BS antenna spacing, the more affection for the spatial correlation values is. The optimum set of parameters is $\Delta d_s = 10\lambda$ in the BS and $\Delta d_u = 0.5\lambda$ in the MS.

3. The Channel Coding LDPC Algorithm

3.1. LDPC Coder

Different channel codes are applied to transport channel and control channel where the LDPC can be used. The LDPC code can be maximized in its performance by choosing the optimized rate and length of the base matrix.

3.2. LDPC Decoder

Both soft and hard decision decoding can be used to decode LDPC, soft decoding achieves a much better performance than the report [11]. These different decoding algorithms for LDPC code are given in this part.

3.2.1. Belief propagation-based (BP-based) Algorithm

The LDPC code is coded from the checked matrix $M \times N$, H_{mn} including the N variable node v_n , $n \in X = 0, 1, \dots, N - 1$, M checked node c_m , $c \in Y = 0, 1, \dots, M - 1$, which is connected to the v_n , c_m . The BP algorithm [11] updates the log-Likelihood Ratio (LLR) between the checked nodes and variable nodes at each loop till exceeding the limited loops or finding the original data. The received signal is w_n modulated before feeding to the decoder r_n ($n = 0, 1, \dots, N - 1$). The LLR initial F_n for each bit r_n is calculated by the decoder as:

$$F_n = \log \frac{P_r(w_n = 0|r_n)}{P_r(w_n = 1|r_n)} = \frac{2r_n}{\sigma^2} \quad (7)$$

where $P_r(w_n = 0|r_n)$, $P_r(w_n = 1|r_n)$ are the conditional probability for $w_n = 0$ and $w_n = 1$ at each r_n , respectively; σ^2 is the variance of the AWGN channel. $L_{m \rightarrow n}$ - the output of bit m transmitted from the variable node n to the checked node m , can be seen as below:

$$L_{m \rightarrow n} = 2 \tanh^{-1} \left(\prod_{n' \in B(m) \setminus n} \tanh \left(\frac{L_{n' \rightarrow m}}{2} \right) \right) \quad (8)$$

where $B(m) \setminus n$ is a parameter set of the variance nodes in $B(m) \neq n$. The output LLR at each iteration then is updated and sent from the variable node. However, the hardware implementation of BP algorithm is limited by its complexity due to the continuously hard decision of code bit to prevent to carry out till the maximum iteration.

3.2.2. Minimum-Sum (MS) algorithm

The MS algorithm [11] is the BP simplified by using the approximation method which has the advantage of totally eliminating the noise σ^2 . That is, the MS decoder can be done without the variance estimation. The possible ratio is below and is independent to the σ^2 :

$$F_n = \log \frac{P_r(w_n = 0|r_n)}{P_r(w_n = 1|r_n)} = r_n \quad (9)$$

The $L_{m \rightarrow n}$ is contrived as:

$$L_{m \rightarrow n} = \prod_{n' \in B(m) \setminus n} \text{sign}(L_{n' \rightarrow m}) \times \min_{n' \in B(m) \setminus n} |L_{n' \rightarrow m}| \quad (10)$$

3.2.3. Normalized Minimum-Sum (NMS) algorithm

The MS algorithm has its effectiveness in the high LDPC code rate. The given NMS algorithm [11] resolves the problem of the higher BER in low code rate by adding the normalized variable to minimize the approximate errors in MS algorithm. The LLR from m checked node to n variance node is provided as:

$$L_{m \rightarrow n} = \alpha \times \left(\prod_{n' \in B(m) \setminus n} \text{sign}(L_{n' \rightarrow m}) \times \left(\min_{n' \in B(m) \setminus n} |L_{n' \rightarrow m}| \right) \right) \quad (11)$$

The factor α is normalized parameter for minimizing the error.

3.2.4. Offset minimum-sum (OMS) algorithm

The MS algorithm has its effectiveness in the high LDPC code rate. The OMS algorithm [11] uses the adjustable β at the checking output, the LLR from m checked node to n variance node is obtained as:

$$L_{m \rightarrow n} = \prod_{n' \in B(m) \setminus n} \text{sign}(L_{n' \rightarrow m}) \times \max \left(\min_{n' \in B(m) \setminus n} |L_{n' \rightarrow m}| + \beta, 0 \right) \quad (12)$$

3.2.5. Linear approximation minimum-sum (LAMS) algorithm

This LAMS [11] has lower complexity than BP by using linear approximation to optimize factors. LAMS methods minimize the gap between the output and target code and take advantage of low code rate and high SNR system [11]. LAMS combines OMS and the NMS algorithm which reduce problem of the higher BER in low code rate by adding the normalized variable to minimize the approximate errors in MS, by implementing the two α, β parameters to set the LLR $L_{n' \rightarrow m}$, showed as:

$$L_{n' \rightarrow m} = \prod_{n' \in B(m) \setminus n} \text{sign}(L_{n' \rightarrow m}) \times \max \left(\alpha \times \min_{n' \in B(m) \setminus n} |L_{n' \rightarrow m}| + \beta, 0 \right) \quad (13)$$

We choose the linear factors α, β to impact the magnitude of the LLR, as well as the LLR channel.

4. Simulation in 2×2 MIMO-OFDM System

The MIMO-OFDM system with 2×2 antennas is described in Fig. 4. The data in transmitter is fed to LDPC coder and modulated with two constellations of BPSK. It then goes to the SFBC coder and again is modulated by the OFDM with inserted pilot, IFFT and guard interval. From two transmit antennas, the physical medium is the considered 5G channel modelling simulator.

In the receiver, basically, each block has opposite function as the transmitter. The signal is demapped from two receive antennas then demodulated by OFDM method by removing the pilot, guard interval and FFT process. After demodulation, it goes to Wiener Interpolation estimation applied to the MIMO-OFDM receiver to estimate the coefficient of the channel based on the pilot estimation in both time and frequency domain. For channel estimation methods, Wiener interpolation is the most effective approach compared to Linear and Sinc interpolation because it minimizes the expected squared error. The MMSE equalizer is used to minimize the mean square error. The signal now is fed to LDPC decoder by employing the decoding OMS, LAMS and BP-based algorithms to gain the system performance. For the LAMS decoding, we choose the factors α, β as the value of 0.8 and -0.2 , respectively as obtained set of parameters in [11].

The parameters for simulation of 2×2 MIMO-OFDM are depicted in Table 4 with the RMA environment in NLOS propagation at 6 GHz. The shape of the channel transfer function in RMA environment in Fig. 5 has obeyed the Rayleigh distribution. The first lowest path loss is 4.6×10^{-5} at the 150th carrier-wave. The highest pathloss is 0.011 at the 3343th carrier-wave. We use this scenario to deploy our simulation of channel coding in MIMO-OFDM system.

The obtained BER results from different 5G decoding algorithms like OMS, LAMS and BP-based are in Fig. 6. We deployed the correlation coefficient channel in two cases of antenna element spacings in both sides ($\Delta d_s = 10\lambda$; $\Delta d_u = 0\lambda$) and ($\Delta d_s = 30\lambda$; $\Delta d_u = 0.5\lambda$) in MIMO-OFDM system with Wiener estimation method in the receiver, each decoding method is run in just 100 loops.

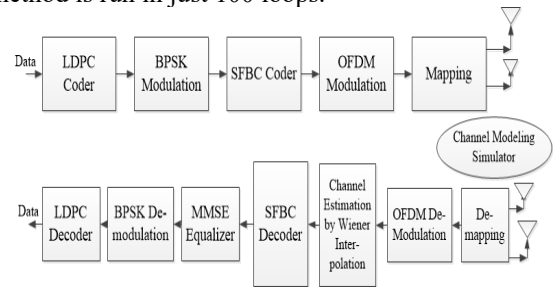


Fig. 4. The transmitter and receiver of 2×2 MIMO-OFDM system

Table 4. Parameters of MIMO-OFDM system

Name	Parameters
Environment	RMa
Transmission	NLOS
Frequency	6 GHz
Bandwidth	20 MHz
Distance of carrier wave	60 KHz
No of sub-Carrier	512
Modulation	QPSK
No of OFDM symbol	114
LDPC	1 or 2
Code rate	1/5

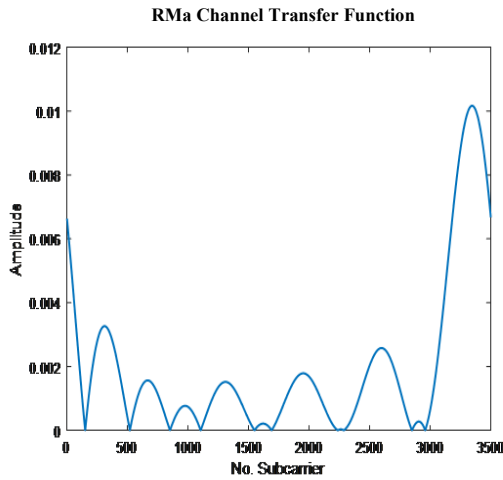


Fig. 5. The transfer function of RMa

In the three decoding methods, with $\Delta d_s = 10\lambda$; $\Delta d_u = 0\lambda$, at $SNR = 0dB$, BP-based decoder has the lowest BER 0.3182 while LAMS decoder has its BER nearest with BP-based, 0.322, and OMS algorithm has the highest BER, about 0.3687. With $\Delta d_s = 30\lambda$; $\Delta d_u = 0.5\lambda$ at $SNR = 0dB$, BP-based decoder has the lowest BER 0.3073 while LAMS has its BER at 0.32 and OMS algorithm has the highest BER, about 0.3329. The BP-based is expressed by the *tanh* function while the OMS and LAMS are used by the *sign* function. For high iteration, OMS and LAMS need to calculate and update in each loop, therefore, the BP-based gains the best system performance. With $SNR = 4dB$, Table 5 shows BERs in two cases of spatial correlation.

From simulation results, with increasing the distance of BS antennas, the MIMO system's performance is better. That is the spatial correlation affects the efficacy of LDPC decoding algorithms. The differential of BER between LAMS and BP-based algorithms is about 0.0296 to 0.0297. As mentioned above, the BP-based is hard for deploying the hardware, while LAMS has lower complexity and more optimization for low code rate in comparison to BP-based. Consequently, we propose to use the LAMS algorithm for decoding the LDPC code in our spatial correlated MIMO-OFDM system.

Table 5. BER of decoding LDPC Algorithm in RMa

SNR	Δd_s ; Δd_u	OMS	LAMS	BP
4 dB	10 λ ; 0 λ	0.2873	0.2247	0.195
	30 λ ; 0.5 λ	0.2397	0.2086	0.179

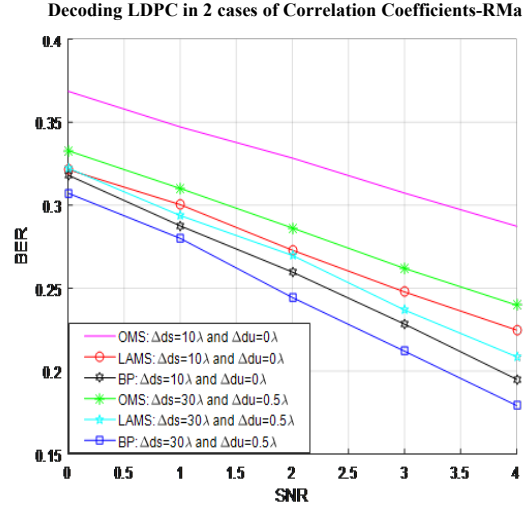


Fig. 6. Deploying LDPC decoding algorithms in MIMO-OFDM system

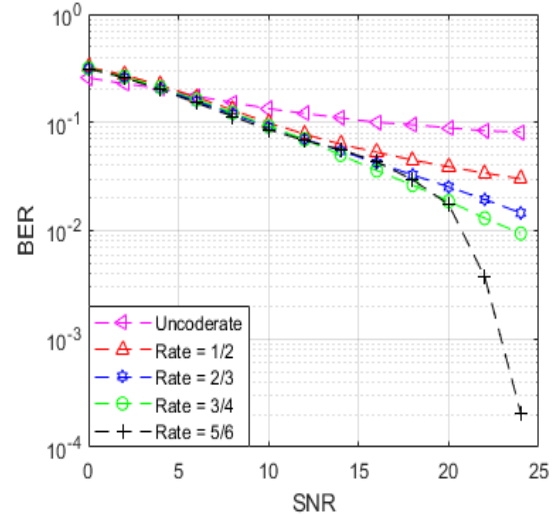


Fig. 7. Deploying LAMS-LDPC algorithms with different code rates in RMa MIMO-OFDM system

As can be seen from Fig. 7, we compare the LAMS LDPC decoding with no code rate (No CR) and code rate (CR) in RMa scenarios in case of $\Delta d_u = 0.5\lambda$ and $\Delta d_s = 16\lambda$. With the block code of 2304 bits, the increasing of the code rate, the decreasing of the BERs that leading to better system performance. At $SNR = 24 dB$ with coded rate of 5/6, the lowest BER is 2×10^{-4} while that of uncode-rate is 0.081. The obtained BERs equivalent to the SNRs are plotted in Table 6.

Table 6. BERs with different code rate of LAMS Decoding in MIMO-OFDM system

SNR	0 dB	8 dB	16 dB	20 dB	24 dB
No CR	0.258	0.153	0.100	0.089	0.081
CR 1/2	0.324	0.130	0.053	0.039	0.030
CR 2/3	0.314	0.119	0.043	0.025	0.015
CR 3/4	0.317	0.123	0.036	0.019	0.009
CR 5/6	0.313	0.114	0.043	0.017	0.0002

Table 7. BER of LAMS-LDPC in distinct code rate and spatial correlation in RMa

SNR	$\Delta d_s; \Delta d_u$	Code rate 2/3	Code rate 5/6
24 dB	$10\lambda; 0\lambda$	0.0118	0.0047
	$10\lambda; 0.5\lambda$	0.0097	0.000038
	$16\lambda; 0.5\lambda$	0.0113	0.00069
	$30\lambda; 1\lambda$	0.0106	0.00062

5. Conclusion

We examined the spatial cross-correlation properties of 5G channel modeling in 2×2 MIMO system in the scenarios of UMi, RMa and InH NLOS cells at 6 GHz frequency band. Based on the built formulae, we derive the minimum correlation value at each MS, BS side by the distances of antenna elements. By exploiting the 5G LDPC channel decoding techniques in spatial correlation conditions, our research evaluates the MIMO-OFDM system's performance. The more the spacings of BS antenna elements, the more effective LDPC channel decoding is applied. In the LDPC decoder algorithms in our correlated system, BP-based is manifested with optimum effectiveness however LAMS algorithm has gained lower complexity than BP-based. For a higher code rate, the effect of LAMS - LDPC decode becomes better. Thus, we propose to use this optimized LAMS decoding, especially in high code rate, in our spatial correlated 5G MIMO system.

Acknowledgments

This research is supported by Hanoi University of Science and Technology (HUST) under Grant T2021-PC-015.

References

1. Thu Nga Nguyen, Van Duc Nguyen, A performance comparison of the SCM and the onering channel modelling method for MIMO-OFDMA systems, in *Wireless Communications Mobile Computing*, Volume16, Issue17, pp. 3123–3138, 10/2016. <https://doi.org/10.1002/wcm.2730>.
2. ETSI TR 138 901 V14.0.0 5G, Study on channel model for frequencies from 0.5 to 100 GHz (3GPP TR 38.901 version 14.0.0 Release 14), ETSI, Tech. Rep, 5/2017.
3. C. -X. Wang, J. Bian, J. Sun, W. Zhang, M. Zhang, A survey of 5G channel measurements and models, in *IEEE Communications Surveys & Tutorials*, vol. 20, no. 4, pp. 3142-3168, Fourth quarter 2018. <https://doi.org/10.1109/COMST.2018.2862141>.
4. Eldowek, B.M., Abd El-atty, S.M., El-Rabaie, ES.M. *et al.*, 3D modeling and analysis of the space-time correlation for 5g millimeter wave MIMO channels. *Wireless Pers Commun* 104, pp. 783–799 (2019). <https://doi.org/10.1007/s11277-018-6051-4>.

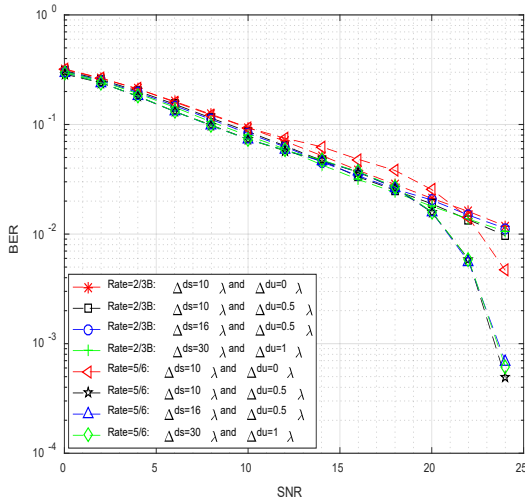


Fig. 8. LAMS-LDPC decoding in spatial correlation MIMO-OFDM system

Fig. 8 is the performance of MIMO system when combining the spatial correlation and the code rate of LAMS decoding algorithm in RMa. As one can be seen, the system performance of the MIMO is better with higher LDPC decoding code rate. With code rate 5/6, when changing the distance of BS antenna elements, BERs vary, however the deviations are negligible.

According to BER analysis, consequently, the influence of the spatial correlation is inconsiderable compared to the impact of the code rate. The smallest acquired BER is derived by the optimum parameter of $\Delta d_s = 10\lambda$ and $\Delta d_u = 0.5\lambda$. This is also the optimum parameter in the case of the code rate 2/3. For code rate 5/6 and with the optimum distance of antenna elements on both sides, the system performance in the case of LAMS is the best. The BER is attained in Table 7 by combining the LDPC decoding code rates and the spatial correlation in MIMO-OFDM system.

5. M. K. Samimi, S. Sun, T. S. Rappaport, MIMO channel modeling and capacity analysis for 5G millimeter-wave wireless systems, 2016 10th European Conference on Antennas and Propagation (EuCAP), 2016, pp. 1-5. <https://doi.org/10.1109/EuCAP.2016.7481507>.
6. Y. Yu, P. J. Smith, P. A. Dmochowski, J. Zhang and M. Shafi, 3D vs. 2D channel models: Spatial correlation and channel capacity comparison and analysis, 2017 IEEE International Conference on Communications (ICC), 2017, pp. 1-7. <https://doi.org/10.1109/ICC.2017.7996405>.
7. K. Haneda *et al.*, Indoor 5G 3GPP-like channel models for office and shopping mall environments, 2016 IEEE International Conference on Communications Workshops (ICC), 2016, pp. 694-699. <https://doi.org/10.1109/ICCW.2016.7503868>.
8. S. Sun *et al.*, Investigation of prediction accuracy, sensitivity, and parameter stability of large-scale propagation path loss models for 5g wireless communications, in IEEE Transactions on Vehicular Technology, vol. 65, no. 5, pp. 2843-2860, May 2016. <https://doi.org/10.1109/TVT.2016.2543139>.
9. 3GPP- TR 25.996 V10.0.0. Technical specification group radio access network spatial channel model for MIMO simulation, 3/2011.
10. T. Richardson, S. Kudekar, Design of low-density parity check codes for 5G new radio, in IEEE Communications Magazine, vol. 56, no. 3, pp. 28-34, March 2018. <https://doi.org/10.1109/MCOM.2018.1700839>.
11. X. Wu, M. Jiang, C. Zhao, Decoding optimization for 5G LDPC codes by machine learning, in IEEE Access, vol. 6, pp. 50179-50186, 2018. <https://doi.org/10.1109/ACCESS.2018.2869374>.
12. Jinghu Chen, M. P. C. Fossorier, Near optimum universal belief propagation based decoding of low-density parity check codes, IEEE Transactions on Communications, vol. 50, no. 3, pp. 406-414, Mar 2002. <https://doi.org/10.1109/26.990903>.
13. S. S. Eldin, M. Nasr, S. Khamees, E. Sourour, M. Elbanna, LDPC coded MIMO OFDM-based IEEE 802.11n wireless LAN, 2009 IFIP International Conference on Wireless and Optical Communications Networks, 2009, pp. 1-5. <https://doi.org/10.1109/WOCN.2009.5010560>.
14. Y. Xin, S. A. Mujtaba, T. Zhang and J. Jiang, Bypass decoding: a reduced-complexity decoding technique for LDPC-Coded MIMO-OFDM systems, in IEEE Transactions on Vehicular Technology, vol. 57, no. 4, pp. 2319-2333, July 2008. <https://doi.org/10.1109/TVT.2007.912163>.